*Laser Physics, Vol. 12, No. 2, 2002, pp. 463–467.*




# Dynamic Dressing of $H_2^+$ in Intense Photon Fields

**L. J. Frasinski, C. R. Courtney, and K. Codling**

*J. J. Thomson Physical Laboratory, the University of Reading, Whiteknights, Reading, RG6 6AF UK*

e-mail: L.J.Frasinski@reading.ac.uk

Received October 11, 2001

**Abstract**—The mechanisms of bond hardening, zero-photon dissociation and orthogonal, counterintuitive alignment that occur when $H_2^+$ ions are exposed to intense femtosecond laser pulses are described in terms of dynamic dressing of the molecular ion system in a photon field. An adiabatic variability is added to the static Floquet picture and the validity of this modification is assessed using the Landau–Zener formula for the probability of non-adiabatic transitions. Application of the dynamic dressing model to the control of chemical reactions is discussed briefly.

Exposing the $H_2^+$ ion to intense femtosecond laser pulses reveals the surprisingly rich dynamics of this simplest of molecular systems. While numerical integration of the time-dependent Schrödinger equation can replicate the experimental data, the best physical insight is obtained by considering $H_2^+$ dressed in a photon field. In the molecular context, this picture allows one to separate the electronic and nuclear motion in the presence of a strong oscillating field [1], and now is known as the Floquet theory (see, for example, *Topical Review* [2]). In this picture the molecular energy curves are repeated at integer numbers of the photon energy and this produces multiple crossings. As the laser intensity increases, the curve crossings become anticrossings and this yields a new set of molecular curves. In principle, these new curves are only adiabatically correct but, in practice, the nuclear dynamics mostly follows the curves on a tens-of-femtosecond timescale. We call this process *dynamic dressing* and argue that it provides a consistent explanation of several phenomena observed recently in $H_2^+$ [3–5].

## BOND HARDENING

In the experimental observation of bond hardening (BH) [3], chirped pulses from a Ti:sapphire laser were amplified to 10 mJ in energy and compressed to about 50 fs duration at a repetition rate of 10 Hz (see [6] for a recent review of high power ultrafast lasers). The pulse bandwidth had an almost perfect Gaussian shape centered at 792 nm and an extent of 22 nm, full width at half maximum (FWHM). The pulse length was varied by scanning the separation of the two compressor gratings and introducing some uncompensated chirp. The linearly polarized beam, 5 mm in diameter, was focused in an ultra high vacuum chamber using an *f*/4 parabolic mirror to give a peak intensity of the order of $10^{14}$ W/cm$^2$. Hydrogen gas was introduced into the vacuum chamber via simple effusion, raising the ambient pressure to about $10^{-6}$ Torr. Following the process of multiphoton ionization of $H_2$, an external electric field directed "forward" and "backward" fragment ions into a vertical, 13 cm-long drift tube. Ions were detected by microchannel plates with a 10-mm circular restriction in front to improve the energy and angular resolutions. The ion time-of-flight (TOF) spectrum and pulse energy were recorded at each laser shot by a digital oscilloscope and stored in a computer.

Potential energy curves for $H_2^+$ dressed in the photon field are shown in Fig. 1. It is sufficient to consider only the two lowest molecular ion states: the attractive $1s\sigma_g$ and repulsive $2p\sigma_u$ states. Since the system, $H_2^+$ plus photons, must be considered as a whole, the molecular curves must be repeated at all discrete energies of the photon field. Zero energy is set at some arbitrarily large number of photons, $N$, and the states are labelled with $(N - n)\omega$, where $n$ is the number of photons absorbed. Due to selection rules, the photon interaction couples only half of the states, alternating between $1s\sigma_g$ and $2p\sigma_u$ for even and odd $n$, respectively. These diabatic states, shown in Fig. 1 as solid lines, describe the system correctly at low laser intensity. When the intensity increases, the curve crossings become anticrossings and a widening of the energy gap between the upper and lower branches of the new, adiabatic states (broken lines) occurs.

On the lower branch the electronic charge oscillates in phase with the laser field, decreasing the energy of the system; on the upper branch these oscillations are in antiphase. At the center of the gap almost the entire electronic charge oscillates between the two protons. As the system moves away from resonance, the amount of oscillating charge diminishes, reflecting the reduced mixing of the $1s\sigma_g$ and $2p\sigma_u$ states. At the $1\omega$ crossing

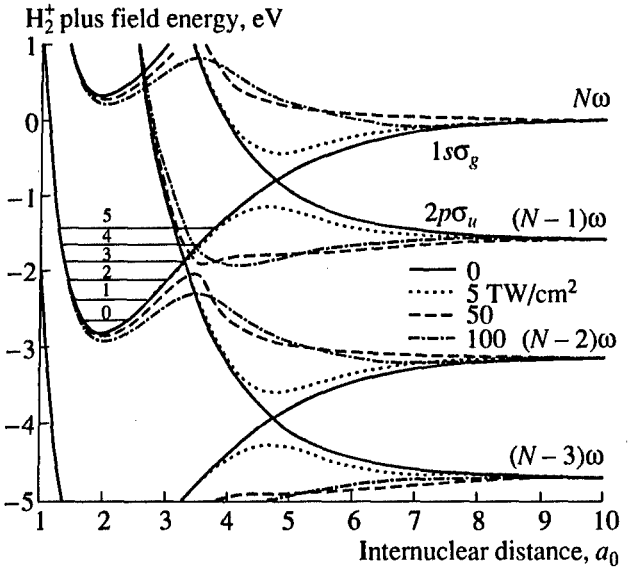


**Fig. 1.** Molecular potential energy curves of $H_2^+$ dressed in a photon field of 792 nm wavelength. With increasing laser intensity curve crossings become anticrossings. A nuclear wave packet with kinetic energy corresponding to the 3rd and 4th vibrational levels of a free molecule can be trapped in the potential well created by intensities above 100 TW/cm$^2$ at $4a_0$.

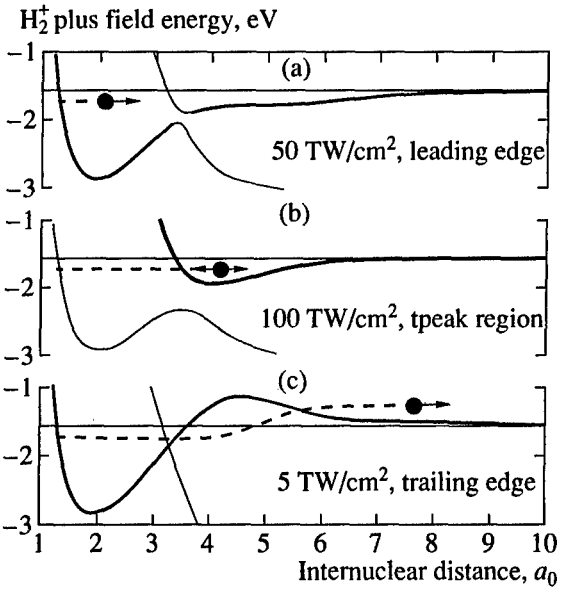


**Fig. 2.** The dynamics of bond hardening. $H_2^+$ is created on the leading edge of the laser pulse and the wave packet jumps the anticrossing gap (a). As the intensity increases, the gap widens and the wave packet is trapped (b). Falling intensity flexes the well upwards and the wave packet is released (c). The kinetic energy release depends on the speed of the intensity fall.

the charge oscillates with the laser frequency; at the $3\omega$ crossing the charge oscillations are three times faster. Strictly speaking, this adiabatic picture is valid only for a slowly evolving system. Nevertheless, it allows us to understand the dynamics of $H_2^+$ on a time scale an order of magnitude slower than the oscillations of the laser field.

In Fig. 2 the BH process is illustrated with the relevant potential curves copied from Fig. 1. The ionization of the neutral molecule starts at about 50 TW/cm$^2$ on the leading edge of the laser pulse, creating a wave packet composed of a few of the lowest vibrational states of $H_2^+$. The interesting part of this wave packet has an energy just below the $(N-1)\omega$ dissociation limit (see Fig. 2a). It crosses the potential well in about 10 fs and arrives at the $3\omega$ gap while the gap is still rather small. The Landau–Zener transition probability (see [7] for a convenient formula) tells us that most of the wave packet crosses the gap diabatically. The wave packet slows down in the shallow part of the potential well, turns back and arrives again at the $3\omega$ crossing, when the gap is much wider and the probability of a diabatic crossing is much smaller. Now the wave packet is trapped in the laser-induced adiabatic state (see Fig. 2b), essentially completing the BH process.

Of particular interest is the decay of the BH state. As the intensity falls on the trailing edge of the laser pulse, the shape of the potential energy curve changes from concave to convex (see Fig. 2c); it now becomes the bottom part of the $1\omega$ anticrossing. In this process the trapped wave packet is lifted up and about a half of it falls back into the $1s\sigma_g$ well, but the other half spills out to the $(N-1)\omega$ dissociation limit. Clearly, the faster the intensity fan time, the higher the wave packet is lifted and the larger is the kinetic energy it gains. Chirping the pulses provides a simple means of varying their fall time and shifting the proton kinetic energy [3].

It is interesting to note the complex *electron* dynamics of the BH state, which is the result of the combined mixing of the $1s\sigma_g$ and $2p\sigma_u$ states at the $1\omega$ and $3\omega$ frequencies. At large internuclear distances the electron charge oscillates in phase with the laser field and the attractive force of the bond comes from the diminishing of these oscillations with increasing internuclear distance. At small distances the charge oscillations become three times faster and in antiphase, but the repulsive force on the nuclei is dominated by the antibonding nature of the $2p\sigma_u$ state.

Energy conservation deserves a brief comment. The dashed trajectory in Fig. 2c indicates that the $H_2^+$ ion gains a fraction of a photon energy in the BH state. This can be explained by absorption of photons from the high-energy end of the spectrum and re-emission at the low-energy end, a dynamic Raman effect within the laser bandwidth (45 meV FWHM).

## ZERO-PHOTON DISSOCIATION

The experimental arrangements to study zero-photon dissociation (ZPD) [4] were the same as in the BH experiment, except that the $H_2$ molecules were exposed to the third harmonic of the Ti:sapphire laser. In one arm of a Mach–Zehnder type setup, a 200 μm thick, type I, BBO crystal generated a laser beam at the second harmonic (400 nm). This was combined with the fundamental in a 300 μm thick, type I, BBO crystal to produce the third harmonic (266 nm) with an energy of up to 60 μJ per pulse. The unwanted longer wavelengths were removed from the beam by dielectric mirrors designed to reflect the third harmonic. The pulse length of approximately 250 fs was determined by cross-correlation with the "fundamental" 50 fs pulses. From the beam and focal properties, the maximum attainable laser intensity was estimated to be about $10^{15}$ W/cm$^2$.

From the ion TOF spectrum, two H + H$^+$ fragmentation channels could be discerned: one of low kinetic energy release (KER), 0–0.5 eV, and one of high KER, near 3 eV. The latter is associated with a vibrational wavepacket travelling along the lower adiabatic potential curve in Fig. 3. The process, called bond softening (BS) [8], is accompanied by the net absorption of one photon. This follows from the fact that the wavepacket starts on a state dressed with $N$ photons and ends on a state dressed with $N-1$ photons. However, the channel with low KER is attributed to a vibrational wavepacket of $H_2^+$ which is temporarily trapped in the potential well created by the upper adiabatic curve [9]. The curves in Fig. 3 clearly show that the well becomes shallower for higher laser intensities. Thus the wavepacket partially escapes as the bottom of the well is pushed upwards in response to an increase in laser intensity on the rising edge of the pulse. If the pulse is not too short, initially trapped population reaches large internuclear separations so that it is not trapped again on the falling edge of the pulse. Since the wavepacket escapes along the $\sigma_g$ state dressed with $N$ photons, no net number of photons is absorbed by the $H_2^+$ ion and hence the term zero-photon dissociation.

Zero-photon dissociation is a signature of vibrational trapping. For $\lambda = 266$ nm, the $v' = 5$ level is the lowest for which trapping can occur. The shaded area in Fig. 3 illustrates that it is the part of the vibrational wavefunction which lies to the right of the one-photon crossing that is trapped. Higher levels are not only trapped more efficiently, but also dissociate more easily via ZPD, due to their vibrational energy. The simultaneous appearance of the slow and the faster protons, suggest that both high and low vibrational levels are populated in $H_2^+$. Then, as soon as the one-photon curve-crossing becomes adiabatic, i.e., at around $10^{13}$ W/cm$^2$ on the leading edge of the laser pulse, a wavepacket originating from the high levels dissociates

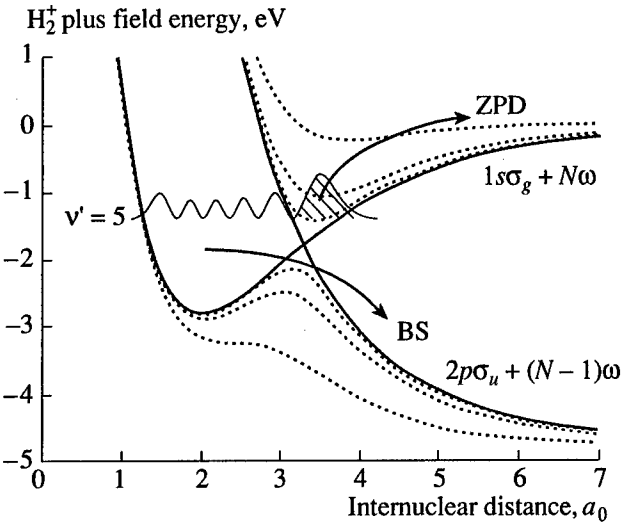


**Fig. 3.** The solid curves represent the $\sigma_g$ state of $H_2^+$ dressed with N photons at $\lambda = 266$ nm and the $\sigma_u$ state dressed with $N-1$ photons. Adiabatic potentials at 0.5, 2, and $10 \times 10^{13}$ W/cm$^2$ are indicated by the dotted curves. The bond-softening channel stems from a vibrational wavepacket following the lower adiabatic potential curves, thereby absorbing one photon. The $H_2^+$ molecule can also be trapped in the laser-induced well above the crossing of the dressed states. An increase in laser intensity makes the well shallower, resulting in zero-photon dissociation.

partially through the process of ZPD, whilst a wavepacket from the levels around $v' = 3$ dissociates exclusively via bond softening.

Adhering to our model of gentle evolution introduced into the Floquet picture, we can reasonably expect that the energy extracted from the field in the dynamic Raman effect is shared among all of the photons, giving a modest red-shift of no more than 1%, i.e., within the bandwidth of the laser. It would be interesting to see if this heuristic estimate can be supported by a rigorous quantum calculation of the photon spectrum.

## ORTHOGONAL ALIGNMENT

The experimental arrangements to study orthogonal alignment [5] were the same as in the zero-photon dissociation experiment, except that the polarization plane of the laser beam could be rotated using a half-wave plate. Ion TOF spectra and pulse energies were recorded for each laser shot and for a range of half-wave plate positions, and stored in a computer.

Figure 4, in a similar way to the previous figure, shows the $1s\sigma_g$ state dressed by a large number of photons, $N$, and the $2p\sigma_u$ state with one photon less, which is absorbed from the field. At low laser intensities the two curves remain basically unperturbed, representing diabatic states crossing at the 1-photon resonance (dashed lines). When the intensity increases, the curve

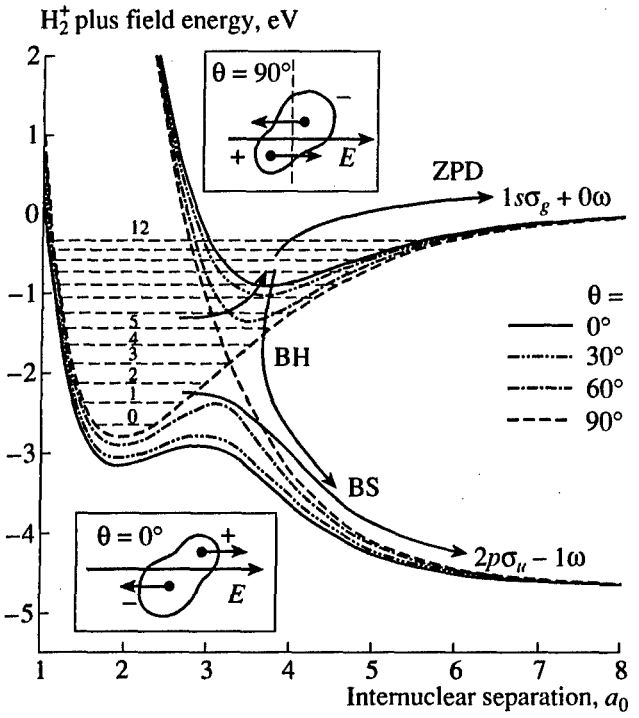


**Fig. 4.** Potential energy curves of $H_2^+$ dressed in a photon field of 266 nm wavelength and $5 \times 10^{13}$ W/cm$^2$ intensity. Lower vibrational levels dissociate via bond softening (BS), where the laser $E$-field effectively pulls the molecule into parallel alignment (lower box). Higher vibrational levels can be trapped in the bond-hardened (BH) state on the upper branch of the anticrossing, where the $E$-field induces a counterintuitive, negative polarization and pushes the molecule into orthogonal alignment (upper box). This process is frustrated by the anticrossing gap shrinking as θ approaches 90°, whereupon the system falls onto the lower branch and the alignment is partially reversed.

crossing becomes an anticrossing and an energy gap steadily opens between the upper and lower branches of the new, adiabatic states (dot-dashed and solid lines). At an arbitrary angular position of the molecule, the width of the gap is determined by the "parallel intensity" [10], $I\cos^2\theta$. Therefore the gap can be opened not only by increasing the laser intensity, $I$, but also by rotating the molecule parallel to the $E$-field, as the values of θ indicate in Fig. 4.

The $H_2^+$ population in the higher vibrational levels can be partially trapped in the BH process. Classically, this means that a wave packet of a higher kinetic energy preferentially follows the diabatic route into the upper branch of the crossing. Increasing laser intensity progressively cuts off the return along this route and traps a substantial part of the wave packet above the 1-photon gap, see the first part of the upper path in Fig. 3. This trapped population can now follow two different dissociation routes. A further increase of laser intensity lifts the wave packet and enables it to proceed to the $N\omega$ limit in the ZPD process described before (the upper path). A reduction of the parallel intensity releases the wave packet from the trap, splitting it between the attractive and repulsive diabatic states. The part in the repulsive state immediately dissociates to the $(N-1)\omega$ limit, as indicated. The remaining part of the released wave packet continues to oscillate in the $1s\sigma_g$ potential well but may still have a significant probability of an adiabatic transition to the $(N-1)\omega$ limit through the partially open gap.

The BS channel exhibits sharp a angular distribution along the laser $E$-field, which can be understood in classical terms. The laser field polarizes the molecule (the electronic charge oscillates in phase with the laser field) and exerts a torque that aligns the molecule parallel to the field (see the lower box in Fig. 4).

The BH channel displays a counterintuitive effect that has a quantum mechanical origin. On the upper, BH branch of the anticrossing, the diabatic $1s\sigma_g$ and $2p\sigma_u$ wave functions superpose in such a way that the polarization is negative, i.e., the electronic charge oscillates in antiphase with the laser field. The negative polarization produces a torque that starts to align the molecule orthogonally to the field (see the upper box in Fig. 4). However, the completion of this alignment is frustrated by a reducing energy gap as θ approaches 90° and an increased rate of diabatic transitions to the lower branch of the anticrossing; consequently the alignment is partially reversed. The overall effect is peaking of the BH channel at intermediate angles, reflecting the two opposing processes of alignment.

Rather than considering forces acting on the molecule, one can study potential energy surfaces to explain the alignment dynamics. The anticrossing curves of Fig. 4 create two such surfaces that are functions of internuclear separation and angular position [10, 11]. On either of these surfaces the system seeks a minimum. On the BS surface this corresponds to the dissociation path of maximal *ac* Stark shift, along the 0° direction. On the BH surface the energy minimum is at 90°, where the Stark shift is minimal. However, this minimum is leaky and the system falls down to the BS surface.

## VALIDITY OF DYNAMIC DRESSING

The energy curves in Figs. 1–4 have been calculated by diagonalizing the molecule-field Hamiltonian in the Floquet picture [2], which assumes a *constant* amplitude of the laser field. However, to understand the processes of bond hardening, zero-photon dissociation and orthogonal alignment one has to modify this picture and introduce the notion of *changing* energy curves due to the varying amplitude of the laser field. It is important to investigate the validity of this modification, especially because the energy curves vary considerably on the timescale of tens of femtoseconds—only an order of magnitude slower than the field frequency.

The Landau–Zener probability, $W$, for the diabatic passage of a particle through a curve crossing is given by the following formula [7] (in SI units):

$$W = \exp(-2\pi V_{12}^2/(\hbar v|F_1 - F_2|)), \quad (1)$$

where $V_{12} = \langle 1|e\mathbf{r} \cdot \mathbf{E}(t)|2\rangle = \hbar\omega_R/2$ is the off-diagonal element of the interaction Hamiltonian that couples the diabatic states 1 and 2, $e\mathbf{r}$ is the electric dipole-moment operator, $\mathbf{E}(t)$ is the laser field, $\omega_R$ is the Rabi frequency ($\hbar\omega_R$ gives the energy gap between the adiabatic branches of the anticrossing), $F_i = dU_i/dR$ are the slopes of the two diabatic energy curves at the crossing, and $v$ is the velocity of internuclear motion. Considering the difference of the diabatic curves, $U = U_1 - U_2$, we can write $v|F_1 - F_2| = |dR/dt||dU/dR| = |dU/dt|$. The $dU/dt$ term can be interpreted as the potential energy variation experienced by a particle moving along stationary curves.

To describe a particle sitting at a fixed internuclear separation on a changing adiabatic curve, we interpret the $dU/dt$ term as the variation in the potential energy difference between the two adiabatic branches. In the worst-case scenario, this energy variation is fastest at the crossing and is equal to the gap opening (or closing) speed: $dU/dt = \hbar d\omega_R/dt$. Substituting these results in (1) one obtains the probability of the particle jumping from one branch of the anticrossing to the other one due to the varying size of the gap:

$$W = \exp(-\pi\omega_R^2/|d\omega_R/dt|). \quad (2)$$

This formula allows one to calculate deviations from the assumed adiabacity. They are expected to be largest in the BH experiment, where the $3\omega$ gap is small and the pulses short. Looking at Fig. 1, this gap is no less than 0.1 eV and varies no faster than 0.1 eV/10 fs. The corresponding Rabi frequency is $\omega_R = e/\hbar \times 0.1$ eV = 0.15 rad/fs, which gives $W \le \exp((-\pi 0.15^2/(0.15/10)) < 1\%$. This means that the dynamic dressing model provides an accurate description of the experiments discussed above. Moreover, this suggests a useful rule of thumb: *A molecule exposed to a laser pulse of tens of femtoseconds duration follows the adiabatic curve if the energy gap is open to at least 0.1 eV.*

## CONTROL OF CHEMICAL REACTIONS

Finally, let us suggest an application of the dynamic dressing model. The essence of controlling chemical reactions is the ability to steer the evolution of nuclear wavepackets in energy, internuclear separation and angular position. The dynamic dressing mechanism influences all of these degrees of freedom. The dynamic Raman effect allows one continuous control of wavepacket energy, without the need to vary the wavelength. Instead, a particular choice of wavelength can be used to create trapping in a bond-hardened state at a specific internuclear separation. The control of angular position of the molecule can be effected by switching between bond softening and bond hardening, thereby inducing, respectively, parallel or orthogonal alignment, relative to the laser $E$-field.

## REFERENCES


1. Fedorov, M.V., Kudrevatova, O.V., Makarov, V.P., and Samokhin, A.A., 1975, *Opt. Commun.*, **13**, 299.
2. Giusti-Suzor, A., Mies, F.H., DiMauro, L.F., Charron, E., and Yang, B., 1995, *J. Phys. B: At. Mol. Opt. Phys.*, **28**, 309.
3. Frasinski, L.J., Posthumus, J.H., Plumridge, J., Codling, K., Taday, P.F., and Langley, A.J., 1999, *Phys. Rev. Lett.*, **83**, 3625.
4. Posthumus, J.H., Plumridge, J., Frasinski, L.J., Codling, K., Divall, E.J., Langley, A.J., and Taday, P.F., 2000, *J. Phys. B: At. Mol. Opt. Phys.*, **33**, L563.
5. Frasinski, L.J., Plumridge, J., Posthumus, J.H., Codling, K., Taday, P.F., and Langley, A.J., 2001, *Phys. Rev. Lett.*, **86**, 2541.
6. Backus, S., Durfee III, C.G., Murnane, M.M., and Kapteyn, H.C., 1998, *Rev. Sci. Instrum.*, **69**, 1207.
7. Zavriyev, A. and Bucksbaum, P.H., 1994, *Molecules in Laser Fields*, Bandrauk, A.D., Ed. (New York: Marcel Dekker).
8. Bandrauk, A.D. and Sink, M.L., 1981, *J. Chem. Phys.*, **74**, 1110.
9. Giusti-Suzor, A. and Mies, F.H., 1992, *Phys. Rev. Lett.*, **68**, 3869.
10. Zavriyev, A., Bucksbaum, P.H., Muller, H.G., and Schumacher, D.W., 1990, *Phys. Rev. A*, **42**, 5500.
11. Bandrauk, A.D. and Turcotte, G., 1983, *J. Phys. Chem.*, **87**, 5098.